MASSACHUSETTS INSTITUTE OF TECHNOLOGY
LINCOLN LABORATORY

A THEORY FOR OPTIMAL MTI DIGITAL SIGNAL PROCESSING
PART I. RECEIVER SYNTHESIS

R. J. McAULAY

Group 41

TECHNICAL NOTE 1972-14
(Part I)

22 FEBRUARY 1972

LEXINGTON MASSACHUSETTS

The work reported in this document was performed at Lincoln Laboratory, a center for research operated by Massachusetts Institute of Technology, with the support of the Department of the Air Force under Contract F19628-70-C-0230.

A Theory for Optimal MTI Digital Signal Processing
Part I: Receiver Synthesis

ABSTRACT

A classical problem in radar theory is the detection of moving targets in a ground clutter plus receiver noise background. Improvements in clutter rejection have recently been made by replacing analog MTI processors by their digital equivalents as this eliminates many of the problems associated with the maintenance of the analog hardware. In an attempt to determine the ultimate improvements possible using this new technology, the MTI problem was formulated as a classical detection problem and solved using the generalized likelihood ratio test. By manipulating the likelihood ratio, the receiver could be interpreted as a clutter filter in cascade with a doppler filter bank. The performance of the optimum receiver was evaluated in terms of the output signal-to-interference ratio and compared with well-known MTI processors. It was shown that near-optimum performance can be obtained using a sliding weighted Discrete Fourier Transform (DFT).

All of the results in Part I assume uniformly spaced transmitted pulses, which, for high velocity aircraft, leads to aliasing of the target and clutter spectra and detection blind speeds. In Part II the maximum likelihood method is applied using a more general model for the non-uniformly sampled target returns. This leads to an optimum receiver that is a slightly more complicated version of the sliding weighted DFT. In addition to removing the detection blind speeds, it is found that unambiguous doppler measurements are possible by selecting the staggering algorithm to properly design the signal's ambiguity function.

Accepted for the Air Force
Joseph R. Waterman, Lt. Col., USAF
Chief, Lincoln Laboratory Project Office

I. INTRODUCTION AND SYNOPSIS

The exact role of radar in the beacon equipped Air Traffic Control (ATC) system is uncertain, and the issue will probably not be completely resolved until after this decade. In the interim it is quite clear that it will be necessary to employ radar for the detection and tracking of uncooperative non-beacon-equipped aircraft. It is therefore of interest to determine whether or not recent advances in radar technology could have any serious impact in improving the performance of radar as an ATC surveillance sensor.

There are two basic problems associated with the use of radar for aircraft surveillance. The first arises from the fact that the radar uses a fan beam in elevation to obtain the desired altitude coverage. This means that target returns must be processed in a strong ground clutter background, a problem which has not really been successfully resolved even after two decades of MTI development. Once a target return has been detected, there remains the problem of associating the radar position measurement with the aircraft that was the actual source of the datum. The difficulty here arises from the fact that radar has been used to extract information of only the position of the aircraft, no velocity filtering having been performed.

It was originally intended that a study be made of recent advances in radar clutter processing techniques that have resulted mainly through the use of digital signal processing (DSP). On trying to deduce a rational means for determining the enhancement in clutter rejection that might be obtained using DSP in conjunction with the present enroute radars, it was discovered that no general body of theory was available to adequately characterize the signal and noise environment that confronts the MTI processor. Hence no optimal MTI

receivers had ever been derived, hence no performance measures existed for comparing a practical receiver with the theoretically optimum. It was decided that such a theoretical investigation be undertaken, the results of which make up the bulk of this paper. In addition to deriving a theory that puts classical MTI processors in perspective, a new optimal processor is deduced that can lead to significant improvements in the ability to detect targets in ground clutter. Quite accidentally, this processor happens to be capable of resolving the data association problem as it provides for unambiguous estimates of aircraft velocity. These estimates can be used to perform bulk filtering on the raw data and, in addition, lead to significant enhancement of the quality of aircraft tracks. The processor will have to be implemented using DSP techniques which is entirely appropriate considering the current developments in radar technology.

The paper is structured as follows: In Section II models are derived for the sampled-data target and clutter returns that evolve from a particular range-resolution cell as the antenna scans through azimuth. Statistical Decision Theoretical tests are then applied to these models in Section III to derive the optimum detector. It is shown that the optimum receiver consists, not surprisingly, of a clutter rejection filter and a bank of matched filters. The pulse-canceller filters used in classical MTI technology can be interpreted as practical approximations to the optimum clutter rejection filter. The goodness of this approximation is the subject of Section IV where it is shown that the performance of the optimal and suboptimal filters is well-characterized by the signal-to-interference ratio (SIR). This performance measure is used to compare the detection in clutter capabilities of the classical MTI filters

with the optimum processor. It is shown that the two-pulse canceller performs very poorly indeed, and that the ideal clutter notch filter loses 10 dB in detection SNR as compared with the optimum. Since the receiver involves filters that are matched to the two-way antenna pattern the possibility exists for optimum azimuth estimation. The standard formula for the mean-squared error in the delay parameter is applied to the azimuth parameter in Section V. A brief discussion of the effects that weather clutter would have on the optimal ground clutter processor is included in Section VI. For theoretical completeness the optimum weather clutter processor is derived and interpreted in terms of adaptive minimum-mean-squared-error filters.

The results in Part I are based on the assumption that pulses leave the transmitter uniformly spaced in time. For ATC en route L-band radars in which the unambiguous range must be 200 nmi, unambiguous velocity measurements are not possible. Furthermore, "blind speeds" occur at multiples of the transmitter PRF at which the detection SNR of even the optimal detector is degraded below practically useful limits. In the development of classical MTI processing it has been found from intuitive considerations that if the transmitter pulses are staggered in time, improved detection performance can be obtained. However, there has been no theoretical investigation of the exact effect that staggered PRF's have on the underlying target and clutter models. In Part II this question is explored in detail as a signal design problem and uses the analytical techniques developed in Part I.

II. TARGET AND CLUTTER MODELS FOR MTI PROCESSING

The key discriminant that is used to process aircraft targets out of a ground clutter background is the doppler frequency shift that is induced by the aircraft as it moves relative to the stationary clutter. The processing is done on the basis of a set of returns received as the antenna scans past the aircraft. Since the aircraft moves slowly relative to the tip speed of the antenna, there will be no significant change in the target range during the short time on target. For this reason MTI is fundamentally a sampled data system as the relevant information shows up at the same range each interpulse period. Historically pulse-to-pulse processing has been done by storing all of the range data from each transmitted pulse in delay lines. More recently, it has become popular to store samples of the range data and implement the MTI filters digitally, as this overcomes many of the practical problems associated with analog processing. In an attempt to obtain a measure of the clutter rejection capabilities of the best possible MTI processor, digital or analog, it became clear that good performance upper bounds were not available. In an attempt to deduce them, it was also recognized that presently used target and clutter models are imprecise and leave out valuable information that can be used in target tracking. The historical background and development of classical MTI can be found in [1] - [3]. Reference [2] provides the best description of target and clutter models, but fails to include the target azimuth which is also a relevant parameter to be estimated. The general approach to target and clutter modeling and detector synthesis developed in this paper has much in common with the work in reference [4] which documents the results of a parallel but independent study of Airborne MTI.

Target Model

The radar transmits a never-ending sequence of simple on-off pulses of RF energy at carrier frequency f_c Hz. The complex envelope of the basic pulse is p(t), where

$$p(t) = \begin{cases} \sqrt{E_p}/\Delta T & 0 \leqq t \leqq \Delta T \\ 0 & \text{otherwise} \end{cases} \tag{1}$$

E_p being the energy per pulse. The transmitted waveform is therefore

$$\xi_1(t) = e^{j2\pi f_c t} \sum_{n=-\infty}^{\infty} p(t - nT_p) \tag{2}$$

where T_p is the interpulse period. Throughout Part I it is assumed that T_p is constant, while Part II is devoted to studying the effects of changing T_p from pulse-to-pulse. For the Air Route Surveillance Radar (ARSR), the radar to which the results of this study are to be applied, the preceding parameters have values f_c = 1300 MHz and T_p = 1/360 sec.

If an aircraft is located at azimuth φ and the antenna scans at a rate ω_s rad/sec. then the detailed model of the signal return for the conventional scanning pulsed radar [5] is then[1]

$$\xi_2(t) = \gamma G^2(\omega_s t - \varphi)\, e^{j2\pi \nu t} \sum_{n=-\infty}^{\infty} p(t - nT_p - \tau) \quad . \tag{3}$$

In (3) $e^{j2\pi\nu t}$ represents the doppler modulation due to the aircraft motion, $\nu = 2v_r f_c/c$ is the doppler shift (v_r = radial velocity towards the radar,

---

[1] The carrier frequency is removed at the receiver.

c = velocity of light); $G^2(\theta)$ is the antenna two-way voltage gain, τ is the delay corresponding to the target's position at range $R = c\tau/2$, φ is the target bearing and $\gamma = Ae^{j\theta}$ represents the unknown amplitude and phase of the carrier signal return.

For the ARSR the pulse duration $\Delta T = 2\mu$ sec. is small relative to the interpulse period of $T_p = 1/360$ and since the antenna pattern changes slowly relative to ΔT the following approximation can be used:

$$G^2(\omega_s \tau - \varphi) \sum_{n=-\infty}^{\infty} p(t - nT_p - \tau) \approx \sum_{n=-\infty}^{\infty} G^2(\omega_s nT_p + \omega_s \tau - \varphi)\, p(t - nT_p - \tau) \quad . \tag{4}$$

Furthermore at L-band targets moving at 600 knots induce a doppler shift of 2600 Hz. Hence the smallest period of the doppler modulation is .4 msec. which is large relative to ΔT, hence allowing the approximation

$$e^{j2\pi\nu t}\, p(t - nT_p - \tau) \approx e^{j2\pi\nu(nT_p + \tau)}\, p(t - nT_p - \tau) \quad . \tag{5}$$

The constant $2\pi\nu\tau$ can be lumped with the unknown RF phase leaving

$$\xi_3(t) = \gamma \sum_{n=-\infty}^{\infty} G^2(n\omega_s T_p + \omega_s \tau - \varphi)\, e^{j2\pi\nu nT_p}\, p(t - nT_p - \tau) \quad . \tag{6}$$

It is standard practice to match filter each T_p segment of range data to enhance the range resolution. This is accomplished using the filter with impulse response $h(t) = p(-t)/\sqrt{E_p}$ (with delay ΔT to insure realizability). The resulting waveform is

$$S(t; \underline{\alpha}) = \int_0^{T_p} \xi_3(t-\sigma)\, h(\sigma)\, d\sigma$$

$$= \gamma\sqrt{E_p} \sum_{n=-\infty}^{\infty} G^2(n\omega_s T_p + \omega_s \tau - \varphi)\, e^{j2\pi\nu n T_p}\, \psi_p(t - nT_p - \tau) \quad (7)$$

where

$$\psi_p(t) = \frac{1}{E_p} \int_{-\infty}^{\infty} p(\sigma)\, p(\sigma + t)\, d\gamma \quad (8)$$

is the autocorrelation function of the basic pulse and $\underline{\alpha} = (\nu, \varphi)$.

Notice that although $S(t; \underline{\alpha})$ represents a continuous function in range, the effects of the doppler modulation and antenna beam pattern are well approximated by discrete time sample-values taken each interpulse period. In other words the significant changes in the doppler information arise only every T_p sec., hence some provision must be made for storing all of the range information over several T_p segments. In classical MTI this is done using a number of analog delay lines each of length T_p sec. For a variety of reasons that are of more practical interest than theoretical, modern MTI processors have been implemented digitally. This means that each T_p seconds of range data is sampled at discrete range intervals and converted to a digital number for digital processing. It is convenient to think in terms of the data that evolves from a particular range resolution cell on a sampled-data basis. Ideally this sampling would be done at least twice per radar pulse width to prevent a loss in detectability due to sampling rate [6]. In this case a 1 megacycle A/D converter would be needed to sample $S(t; \underline{\alpha})$ in (7) to produce samples spaced $\Delta T/2 = 1\mu$ sec apart.

Henceforth it is assumed that samples of $S(t; \underline{\alpha})$ are taken at times $nT_p + m\Delta T/2$ sec., where first a value of n is specified, and then for each value of n, m = 1, 2, ... , M. The processor can be visualized as having M separate memories and as each range sample is taken it is shuffled to the memory unit whose index corresponds to the range cell being sample.

Therefore in the m^{th} memory unit are stored the samples taken at times $t_n^m = nT_p + \Delta T/2$ which when applied to (7) yields the target sample values

$$S(t_n^m; \underline{\alpha}) = \gamma\sqrt{E_p}\, G^2 (n\omega_s T_p + \omega_s \tau - \varphi)\, e^{j2\pi\nu nT_p} \psi_p\left(\frac{m\Delta T}{2} - \tau\right) \qquad (9)$$

$$n = 0, 1, 2, \ldots, N; \; m = 1, 2, \ldots, M \quad .$$

For convenience it has been assumed that the sample-store operation begins at t = 0 at which time the antenna is pointing in the reference azimuth. Since the exact value of τ is unknown, the factor $\sqrt{E_p}\ \psi_p\left(\frac{m\Delta T}{2} - \tau\right)$ is unknown and adjoined to $|\gamma|$.

Furthermore the antenna pattern changes very slowly relative to a pulse width ΔT, hence

$$G^2(n\omega_s T_p + \tau - \varphi) \approx G^2 (n\omega_s T_p + \omega_s \frac{m\Delta T}{2} - \varphi) \quad . \qquad (10)$$

Since φ, the aircraft azimuth, is unknown, the bias $\omega_s\, m\Delta T/2$ can be included in its definition. However, it will be necessary to add this bias term onto the estimated value of φ.

Therefore when an aircraft is located within the m^{th} range ring, N complex data samples corresponding to one scan of the radar will be stored in

the m^{th} memory unit, whose values are

$$S_n^m(\underline{\alpha}) = \gamma G^2(n\omega_s T_p - \varphi)\, e^{j2\pi\nu nT_p} \qquad n = 0, 1, 2, \ldots, N \ . \tag{11}$$

The vector $\underline{\alpha} = (\nu, \varphi)$ denotes the unknown doppler shift and azimuth location of the aircraft. In the most general context it is desirable to detect the presence of an aircraft and to estimate the parameters ν and φ as well. Equation (11) resembles the classical delay-doppler target model. In this case, however, the delay corresponds to the target bearing. This can be made explicit by defining $\tau = \varphi/\omega_s$, and

$$g(t) = G^2(\omega_s t) \qquad 0 \leqq t \leqq T_s \tag{12}$$

where $T_s = 2\pi/\omega_s$ is the time for one antenna scan, the time needed to collect the N data samples. Then (11) can be written as

$$S_n^m(\underline{\alpha}) = \gamma\, g(nT_p - \tau)\, e^{j2\pi\nu nT_p} \tag{13}$$

$$n = 0, 1, \ldots, N-1; \quad NT_p = T_s$$

where $\underline{\alpha}$ is defined to be tuple (ν, τ). Equation (13) is interesting because it suggests that the optimum filter will probably involve a bank of filters each matched to the two-way antenna pattern, g(t), but tuned to different doppler frequencies. A visual summary of the target model is presented in Fig. 1.

Clutter Model

Since ATC radars use fan beams in elevation to obtain altitude coverage, it will happen that objects at zero elevation will be illuminated by the transmitted pulses and constitute legitimate radar returns. Due to range-gating, only

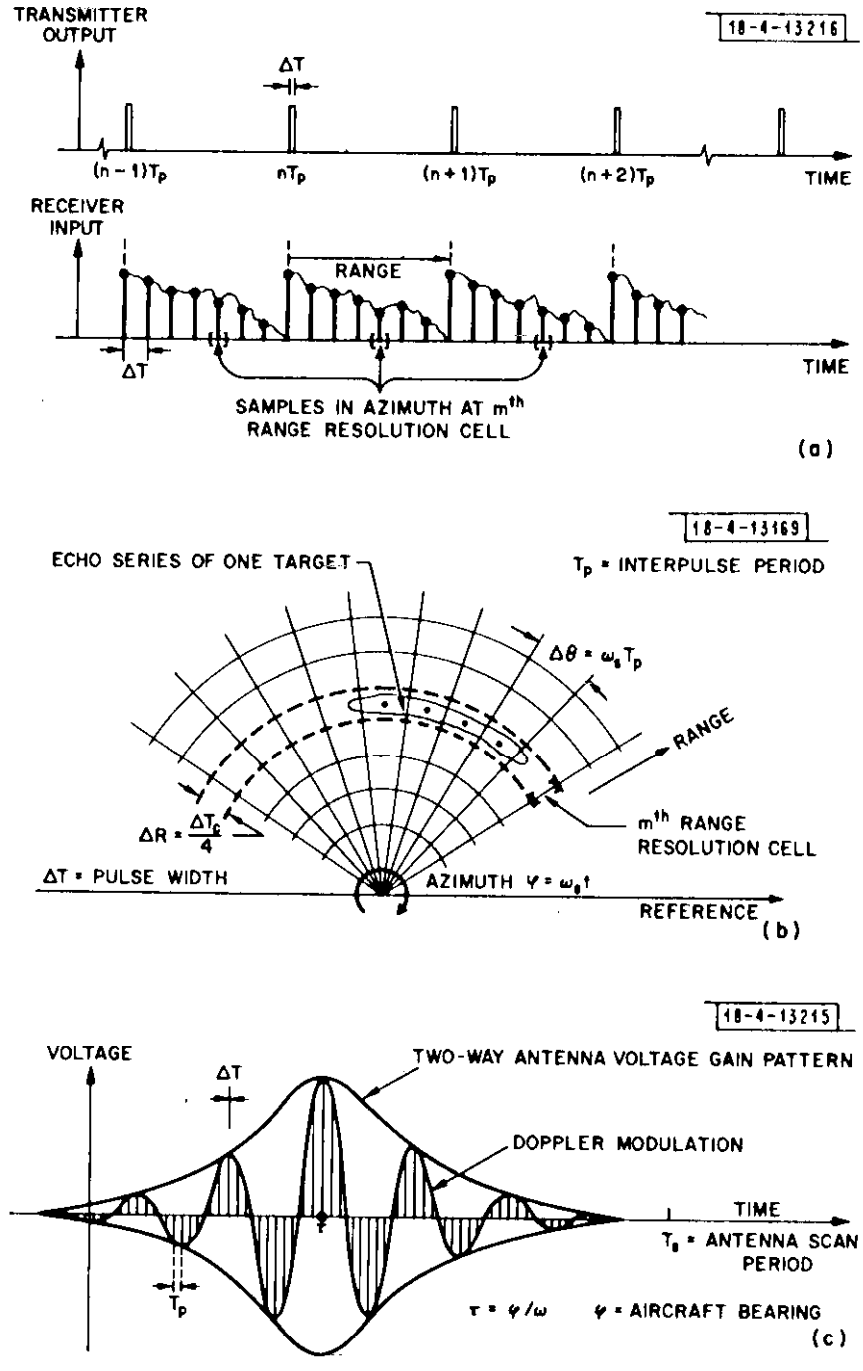

Fig. 1. (a) Sampling pattern in range. (b) Sampling pattern in range and azimuth. (c) Typical voltage samples due to aircraft in m^{th} range ring.

those objects located in the m^{th} range-resolution ring will constitute sources of interference to the target signal, as illustrated in Fig. 2(a). Each scattering center can be considered a target moving with zero velocity. Hence, the k^{th} scatterer in the m^{th} range ring at azimuth φ_k yields a clutter signal return according to (13) with $\nu = 0$, namely

$$C_{k,n}^{m} = \gamma_k \, g(nT_p - \tau_k) \tag{14}$$

where $\tau_k = \varphi_k/\omega_s - m\,\Delta T/2$ takes the bias term $m\Delta T/2$ into account. In this case $\gamma_k = A_k e^{j\theta_k}$ where A_k is related to the scattering cross-section of the k^{th} scatterer and θ_k is the carrier phase shift it introduces. The total clutter return is the aggregate of the signals in (14) and is therefore given by

$$C_n^m = \sum_k C_{k,n}^m = \sum_k \gamma_k \, g(nT_p - \tau_k) \quad . \tag{15}$$

The antenna scanning pattern and transmitter PRF are not synchronized which means that each time the beam returns to the reference azimuth new phase relationships will be generated between the collection of scatterers. This means that on a scan-to-scan basis τ_k, A_k, and θ_k will be random variables which means that C_n^m will be a discrete time random process. It is reasonable to assume that the returns from separate scatterers are statistically independent and that the phases of each of the returns are uniformly distributed. Hence the following conditions are satisfied:

$$\overline{\gamma_k} = 0 \tag{16a}$$

$$\overline{\gamma_k \gamma_j} = 0 \tag{16b}$$

$$\overline{\gamma_k \gamma_j^*} = \sigma_k^2 \, \delta_{k,j} \tag{16c}$$

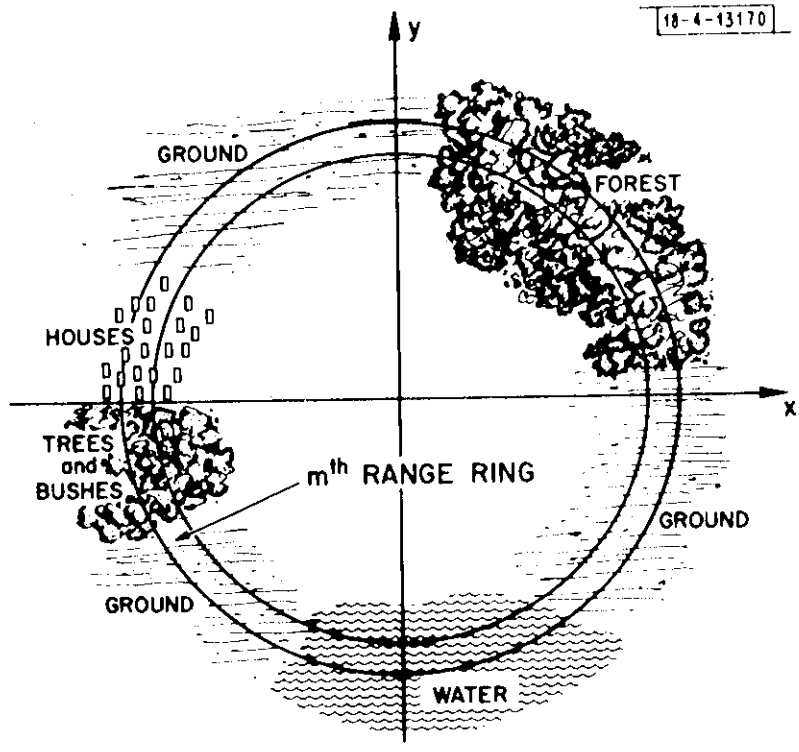

Fig. 2(a). Typical clutter scatterers in a range ring.

where the bar denotes statistical averaging over the ensemble of scatterers. The parameter σ_k^2 is proportional to the radar cross-section of the k^{th} scatterer, and $\delta_{k,j}$ denotes the Kronicker Delta. If it is further assumed that the total number of scatterers is large enough so that some form of the Central Limit Theorem holds, hence C_n^m can be thought of as a sample function of a discrete time complex Gaussian process [7]. Such a process is completely characterized by its mean and two autocorrelation functions. Using (16a) and (16b) it is easy to show that

$$\overline{C_n^m} = 0 \tag{17a}$$

$$\overline{C_n^m C_\ell^m} = 0 \quad . \tag{17b}$$

The final relationship needed is

$$\overline{C_n^m C_l^{m*}} = \sum_k \sum_j \overline{\gamma_k \gamma_j^*}\ \overline{g(nT_p - \tau_k)\ g^*(l\,T_p - \tau_j)} \quad . \tag{18}$$

To evaluate (18) it is noted that the effective time duration of g(t) is well approximated by $T_E = \Delta\theta/\omega_s$ where $\Delta\theta$ is the antenna beamwidth. Hence the number of terms in the summations of (18) will be limited by the number of scatterers in the intervals $(nT_p - T_E/2, nT_p + T_E/2)$ and $(l\,T_p - T_E/2,\ l\,T_p + T_E/2)$, as illustrated in Fig. 2(b). Letting I(n) denote the index set corresponding to the scatterers that contribute non-zero elements to (18) we have

$$\overline{C_n^m C_l^{m*}} = \sum_{k \in I(n)} \sum_{j \in I(l)} \overline{\gamma_k \gamma_j^*}\ \overline{g(n\,T_p - \tau_k)\ g^*(l\,T_p - \tau_j)} \tag{19}$$

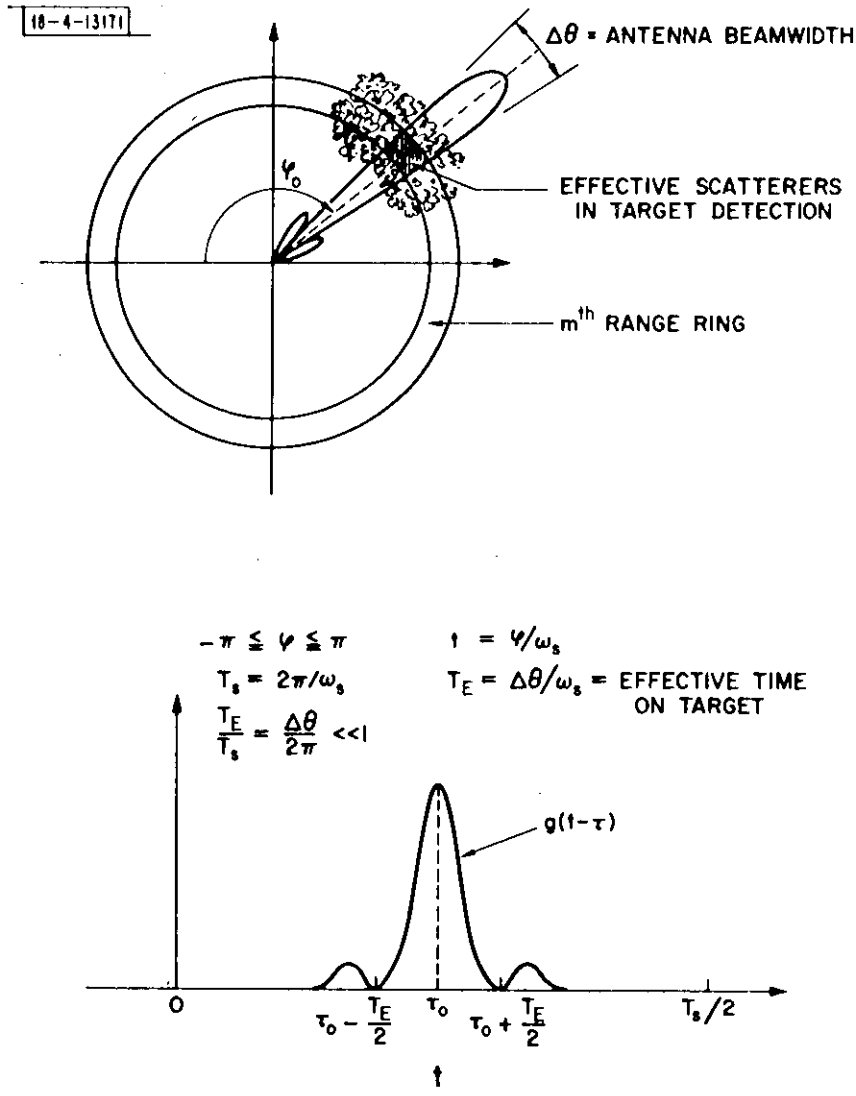

Fig. 2(b). Effective scatterers in a range-azimuth cell.

Since the two-way antenna voltage gain pattern is real and using (16c), (19) becomes

$$\overline{C_n^m C_l^{m*}} = \sum_{k \epsilon I(n)} \sigma_k^2 \, \overline{g(n T_p - \tau_k) \, g(l T_p - \tau_k)} \quad . \tag{20}$$

To carry out the statistical averaging needed to evaluate (20), it is useful to deal with a more general problem.

Consider

$$g(t - \tau_k) \, g(s - \tau_k) = \int_{-T_s/2}^{T_s/2} g(t - \tau_k) \, g(s - \tau_k) \, p(\tau_k) \, d\tau_k \tag{21}$$

where $p(\tau_k)$ is the probability density function of the location of the k^{th} scatterer. It is reasonable to assume that the scatterers are uniformly distributed in azimuth throughout the range ring, in which case

$$p(\tau_k) = 1/T_s \quad . \tag{22}$$

Hence

$$g(t - \tau_k) \, g(s - \tau_k) = \frac{1}{T_s} \int_{-T_s/2}^{T_s/2} g(t - \tau_k) \, g(s - \tau_s) \, d\tau_k \quad . \tag{23}$$

Since the effective time duration of g(t) is small relative to the scan time (i.e., $T_E << T_s$ since $\Delta\theta << 2\pi$), then

$$\int_{-T_s/2}^{T_s/2} g(t-\tau_k)\, g(s-\tau_k)\, d\tau_k \approx \int_{-\infty}^{\infty} g(t-\tau_k)\, g(s-\tau_k)\, d\tau_k$$

$$= \int_{-\infty}^{\infty} g(\sigma + t - s)\, g(\sigma)\, d\sigma$$

$$= R_g(t-s) \tag{24}$$

where $R_g(\tau)$ is the autocorrelation function of the scaled two-way antenna voltage gain pattern. Using (24) with (23) in (20) the correlation between elements in the clutter sequence is given by

$$\overline{C_n^m\, C_l^{m*}} = \frac{1}{T_s} R_g[(n-l)\, T_p] \sum_{k \in I(n)} \sigma_k^2 \,. \tag{25}$$

As the antenna rotates, the beam will envelope ensembles of scatterers whose underlying statistical parameters will be the same over azimuthal segment of the range ring, but may vary from azimuth cell to azimuth cell. This time-varying nature of the average clutter cross-section can be made explicit by defining

$$\sigma^2(nT_p) = \sum_{k \in I(n)} \sigma_k^2 \,. \tag{26}$$

The final expression for the correlation function of the clutter process at the m^{th} range cell is

$$R_c^m(iT_p,\ jT_p) \triangleq C_i^m\, C_j^{m*} = \frac{1}{T_s} R_g\,[(j-j)\, \sigma^2(iT_p) \,. \tag{27}$$

The result shows that the clutter process is basically a non-stationary discrete-time process, due to the time-varying nature of the clutter cross-section. Since the target data evolves as the antenna sweeps past the aircraft, it is intuitively clear that only clutter scatterers that matter are those located within a beamwidth on each side of the target. Over this much smaller interval, the clutter statistics are unlikely to change significantly and it is reasonable to assume that the process is quasi-stationary. In this case $\sigma^2(nT_p)$ can be considered a constant, hence the clutter correlation function reduces to

$$R_c(jT_p) = \overline{C_i^m C_{i+j}^{m*}} = \frac{\sigma^2}{T_s} R_g(jT_p) \quad . \tag{28}$$

Receiver Noise Model

In addition to the target and clutter samples at each range cell, there will be a noise component corresponding to the sampled data version of the receiver noise process. In (7) it was assumed that the signal return after each transmitted pulse was processed by a matched filter and sampled every $\Delta T/2$ sec. out to the maximum range. If $\xi(t)$ represents the RF white Gaussian noise process due to the amplifiers in the receiver front end then its two sided spectrum is

$$S_n(t) = \begin{cases} N_o/2 & |f \pm f_c| \leq B/2 \\ 0 & \text{otherwise} \end{cases} \tag{29}$$

where $N_o = kT_e$, k is Boltzman's constant, T_e the effective temperature and B the bandwidth of the amplifier. Since both amplitude and phase of the signal are to be processed, the receiver noise shows up as a complex Gaussian noise

process. If this is denoted by $\eta(t)$, then its autocorrelation function is

$$\overline{\eta(t)\,\eta^{*}(s)} = 2N_o\,\delta(t-s) \quad . \tag{30}$$

It is this noisy waveform that is processed by the transmitted pulse matched filter to yield to the new noise process

$$w(t) = \int_o^{T_p} \eta(t-\sigma)\,\frac{p(-\sigma)}{\sqrt{E_p}}\,d\sigma \quad . \tag{31}$$

Samples of this process are taken at times $t_n^m = nT_p + m\Delta T/2$, hence

$$w_n^m = \int_o^{T_p} \eta(nT_p + m\Delta T/2 - \sigma)\,\frac{p(-\sigma)}{\sqrt{E_p}}\,d\sigma \tag{32}$$

which represents the noise sample when the m^{th} range resolution cell is sampled at time nT_p. It is easy to show that this complex noise process has zero mean, is Gaussian, and has correlation function

$$\overline{w_i^m\,w_j^{m*}} = 2N_o\,\psi_p\left[(i-j)\,T_p\right] \quad . \tag{33}$$

Since the autocorrelation function of the basic pulse has duration $2\Delta T$ which is small compared to T_p, then it follows that the sampled receiver noise sequence is also a white process, that is

$$\overline{w_i^m\,w_j^{m*}} = 2N_o\,\delta_{ij} \quad . \tag{34}$$

The MTI Problem

Moving Target Indication (MTI) is fundamentally a detection problem. In terms of the signal, clutter and noise models developed in the preceeding

paragraphs it can be stated mathematically as a hypothesis testing problem as follows:

$$H_1^m: \text{target present: } r^m(nT_p) = \gamma\, g(nT_p - \tau)\, e^{j2\pi\nu\, nT_p} + C^m(nT_p) + W^m(nT_p)$$

$$H_0^m: \text{target absent: } r^m(nT_p) = C^m(nT_p) + W^m(nT_p)$$

$$n = 0, 1, \ldots, N-1; \quad m = 1, 2, \ldots, M \tag{35}$$

The notation $r^m(nT_p)$, $C^m(nT_p)$, $W^m(nT_p)$ rather than r_n^m, C_n^m, w_n^m is used to make the sampled-data nature of the problem explicit. The test is to be applied separately to each of the M range-rings. In addition to the lack of knowledge concerning the targets location in range, there also remains the problem of estimating the unknown parameters, γ, ν, τ. In the next section sampled-data techniques are used in conjunction with statistical decision theory to deduce an optimum receiver for target detection and parameter estimation.

III. DECISION THEORY IN MTI AND THE CLUTTER REJECTION FILTER

The detection problem state in (35) could also be formulated as the test for the presence of a finite dimensional signal vector in a colored noise vector background. This is the approach used in [4], [13], [14] and it leads to very useful theoretical results but at some loss to physical insight as the processing is stated in terms of the inverse of a certain clutter correlation matrix. In an attempt to find a solution that can be interpreted in terms of linear filtering theory, the problem formulation will be altered slightly. Since the doppler signal $e^{j2\pi\nu nT_p}$ is amplitude modulated by the two-way antenna pattern $g(nT_p - \tau)$, which is non-zero for a relatively small number of hits compared with N, it can reasonably be assumed that the received signal sequence $r(nT_p)$, is infinite in extent.[2] This sequence is then preprocessed by a sampled-data whitening filter, $h_w(nT_p)$. Denoting the output sequence as $r_w(nT_p)$, then

$$r_w(nT_p) = \sum_{k=-\infty}^{\infty} h_w(nT_p - kT_p)\, r(kT_p) \quad . \tag{36}$$

Under the H_1 hypothesis, the target is absent and

$$r(nT_p) = C(nT_p) + W(nT_p) \quad . \tag{37}$$

This is a discrete-time quasi-stationary random process with correlation function

---

[2] The superscript notation denoting "m^{th} range ring" has been suppressed since identical processing is applied to the data from each range cell.

$$R_r(nT_p) = R_c(nT_p) + 2N_o\ \delta(nT_p) \tag{38}$$

which follows from (28), (34) and the fact that $\delta(nT_p)$ is used to represent the Kronicker Delta δ_{no}. This random process has a spectral density defined as the Z-Transform of its autocorrelation function [7]. If S(z) denotes the spectral density of a sampled-data random process whose correlation function is $R(nT_p)$, then

$$S(z) = \sum_{n=-\infty}^{\infty} R(nT_p)\ z^{-n} = Z\left[R(nT_p)\right] \quad . \tag{39}$$

Applied to (38)

$$S_r(z) = S_c(z) + 2N_o \quad . \tag{40}$$

Since $r_w(nT_p)$ is the result of passing $r(nT_p)$ through a linear filter, its spectral density is [8]

$$S_{r_w}(z) = H_w(z)\ H_w\left(\frac{1}{z}\right)\ S_r(z) \tag{41}$$

where

$$H_w(z) = Z\left[h_w(nT_p)\right] \quad . \tag{42}$$

The filter was to be chosen to generate an uncorrelated output sequence when (37) is the input. This means that

$$S_{r_w}(z) = 1 \tag{43}$$

which can be achieved by choosing the filter so that

$$H_w(z)\ H_w\left(\frac{1}{z}\right) = \frac{1}{S_c(z) + 2N_o} \quad . \tag{44}$$

If $S_c(z)$ were a ratio of polynomials in z, then (44) could be factored into poles and zeros inside and outside the unit circle $|z| = 1$ in the complex z-plane. The poles and zeros within the circle could be assigned to $H_w(z)$, while $H_w(\frac{1}{z})$ would then account for the poles and zeros outside the unit circle. As it turns out, the whitening filter is not used explicitly in the final detector realization, hence it is really not necessary to specify the rule for solving (44). The point is, that under the no signal hypothesis

$$r_w(nT_p) = \eta(nT_p) \tag{45}$$

where $\eta(nT_p)$ is a zero mean, Gaussian discrete time white random process with unity spectral density. Under the H_o hypothesis, the target is present and

$$r(nT_p) = \gamma S(nT_p; \underline{\alpha}) + C(nT_p) + W(nT_p) \tag{46}$$

where from (38) $\underline{\alpha} = (\nu, \tau)$ and

$$S(nT_p; \underline{\alpha}) = g(nT_p - \tau)\, e^{j2\pi\nu nT_p} \quad . \tag{47}$$

The response of the whitening filter to the input (46) is

$$r_w(nT_p) = \gamma S_w(nT_p; \underline{\alpha}) + \eta(nT_p) \tag{48}$$

where

$$S_w(nT_p; \underline{\alpha}) = \sum_{k=-\infty}^{\infty} h_w(nT_p - kT_p)\, S(kT_p; \underline{\alpha}) \quad . \tag{48}$$

An hypothesis test that is completely equivalent to (35) can now be formulated in terms of the detection of a signal in white noise.

$$H_1: \text{target present:} \quad r_w(nT_p) = \gamma S_w(nT_p; \underline{\alpha}) + \eta(nT_p)$$

$$H_0: \text{target absent:} \quad r_w(nT_p) = \eta(nT_p) \quad . \tag{50}$$

For a variety of reasons [5], the optimum detector is chosen as the one that computes a generalized maximum likelihood ratio and compares its value with a threshhold. The target is declared present if

$$\max_{\gamma,\, \underline{\alpha}} \frac{p[r_w(nT_p) | H_o, \gamma, \underline{\alpha}]}{p[r_w(nT_p) | H_1]} > \lambda \quad . \tag{51}$$

When the noise is zero mean, Gaussian and white, (51) is maximized for $\gamma = \hat{\gamma}(\underline{\alpha})$ where[3]

$$\hat{\gamma}(\underline{\alpha}) = \frac{\sum_{n=-\infty}^{\infty} r_w(nT_p)\, S_w^*(nT_p; \underline{\alpha})}{\left[\sum_{n=-\infty}^{\infty} |S_w^*(nT_p); \underline{\alpha})|^2\right]^{\frac{1}{2}}} \tag{52}$$

The denominator in (55) can be considered a normalization factor. Then letting

$$E(\underline{\alpha}) \triangleq \sum_{n=-\infty}^{\infty} |S_w^*(nT_p; \underline{\alpha})|^2 \tag{53}$$

and substituting (52) and (53) into (51) yields the test

$$\max_{\underline{\alpha}} \left| \sum_{n=-\infty}^{\infty} r_w(nT_p)\, S_w^*(nT_p; \underline{\alpha}) \right|^2 / E(\underline{\alpha}) > \lambda \quad . \tag{54}$$

---

[3] The asterisk denotes complex conjugate.

A block diagram representation for this processor is shown in Fig. 3.

This result is still not amenable to physical interpretation and alternate ways of implementing (54) are sought. This will be done following the sampled-data analog of the technique used in [9], [10] in conjunction with the detection of stochastic signals in colored noise. The mathematical manipulations are detailed in the Appendix where it is shown that the test in (54) is equivalent to

$$\max_{\underline{\alpha}} \left| \sum_{n=-\infty}^{\infty} x(nT_p)\, S^*(nT_p;\, \underline{\alpha}) \right|^2 / E(\underline{\alpha}) \tag{55}$$

where now

$$E(\underline{\alpha}) = \sum_{n=-\infty}^{\infty} y(nT_p)\, S^*(nT_p;\, \underline{\alpha}) \tag{56}$$

$$x(nT_p) = Z^{-1}\left[H_w(z)\, H_w(\tfrac{1}{z})\, R(z)\right] \tag{57a}$$

$$y(nT_p) = Z^{-1}\left[H_w(z)\, H_w(\tfrac{1}{z})\, S(z;\, \underline{\alpha})\right] \tag{57b}$$

and $R(z)$, $S(z;\, \underline{\alpha})$ are the z-transforms of the non-whitened sequences $r(nT_p)$, $S(nT_p;\, \underline{\alpha})$, respectively. The sequences $x(nT_p)$ and $y(nT_p)$ can be interpreted as the result of passing signals $r(nT_p)$ and $S(nT_p;\, \underline{\alpha})$ through a filter whose z-Transform is

$$H_c(z) = H_w(z)\, H_w(\tfrac{1}{z}) \quad . \tag{58}$$

From (47) this reduces to

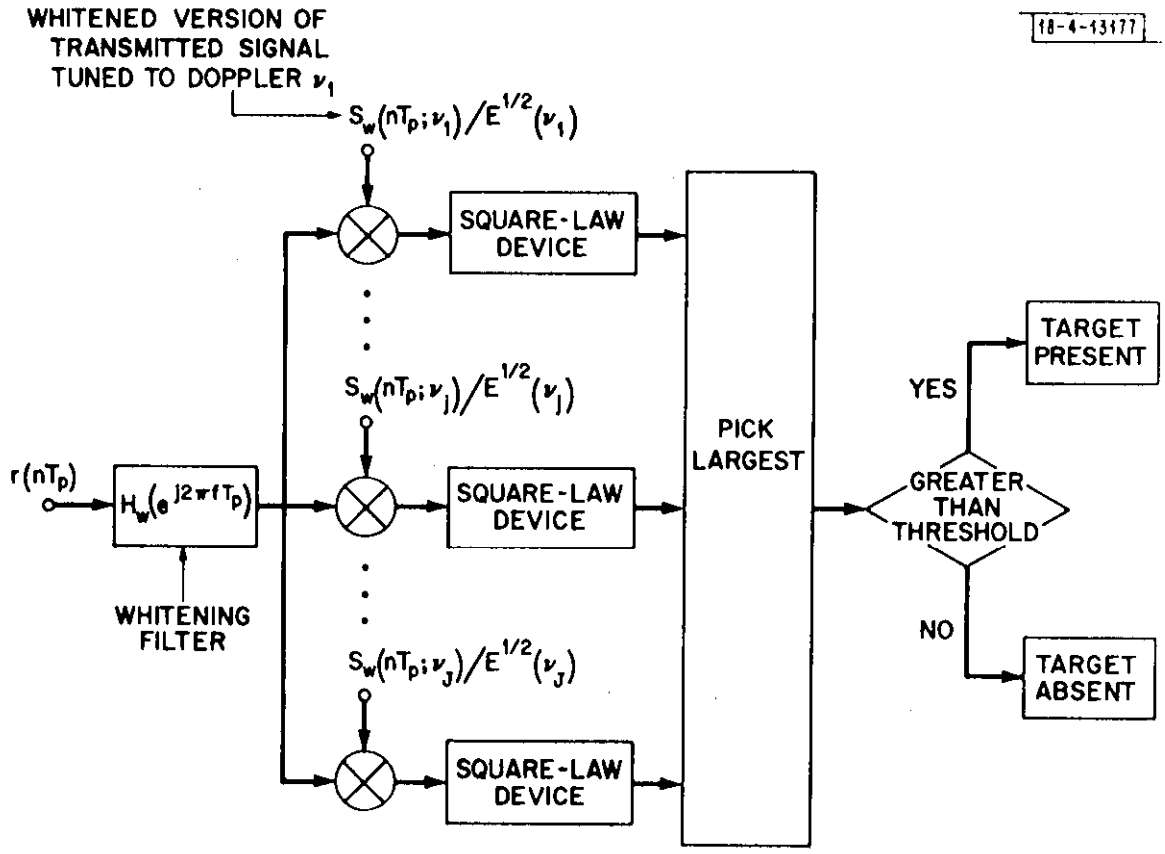

Fig. 3. Block diagram realization of optimum processor using whitening filters.

$$H_c(z) = \frac{1}{S_c(z) + 2N_o} \tag{59}$$

and for reasons that will become clearer as the analysis proceeds, $H_c(z)$ is called the Clutter Rejection Filter. In (57), which is the key operation so far as the detection process is concerned, it is evident that the received signal is filtered by $H_c(z)$, which depends only on the clutter and noise statistics. The output of this filter is then correlated with locally stored versions of the original signal, not the whitened version of that signal. As it is well known that such a correlation operation is optimum for detecting signals in white noise, it appears that $H_c(z)$ is trying to remove the clutter in some optimum way.

Matched Filter Bank

Using (47) and the fact that $E(\underline{\alpha})$ depends only on ν and not on τ (Appendix), it is possible to express (55) in terms of a bank of doppler filters. Defining the impulse reponses

$$h(nT_p;\ \nu) = g(-nT_p)\ e^{j2\pi\nu nT_p}/E^{\frac{1}{2}}(\nu) \tag{60}$$

then it is straightforward to deduce that the likelihood ratio test, (55), is equivalent to

$$\max_{\tau}\ \max_{\nu}\ \Big|\ \sum_{n=-\infty}^{\infty} h(\tau - nT_p;\ \nu)\ x(nT_p)\Big|^2 > \lambda \quad . \tag{61}$$

The argument in (61) is the output at sample time τ (quantized into increments at width T_p) of a filter whose impulse response is tuned to a doppler frequency

ν and matched to the two-way antenna pattern scaled by the factor $E^{\frac{1}{2}}(\nu)$. Therefore at each sample time a search is made over the filter bank for the largest output. Since the memory of the filter is limited by the effective time duration of $g(nT_p)$, T_E, T_E/T_p such values need to be stored. If the largest of these numbers exceeds the threshold then a target is declared present. Furthermore the sampling time and the doppler frequency at which the maximum value occur represent the maximum likelihood estimates of target bearing[4] and velocity.

Therefore a realization for the optimum sampled data MTI receiver has been derived that is intuitively easy to understand from a linear filtering point of view. As shown in Fig. 4, the received samples are processed by a clutter rejection filter that tries to remove the clutter background from the target information. The resulting samples are passed through a bank of filters matched to the original target antenna modulation. These filters further process the target out of the white noise background and at the same time generate estimates of the target bearing and velocity.

The classical works in MTI have focused on only one aspect of the above receiver, namely the realization of the clutter rejection filter. That this is true can be deduced by first noting that the frequency response of a sampled-data filter is given by the z-Transform evaluated on the unit circle. From (60) with $z = e^{j2\pi fT_p}$, the frequency response of the clutter rejection filter is

---

[4] Provided the bias term $\omega_s \Delta T$ is added to the estimate.

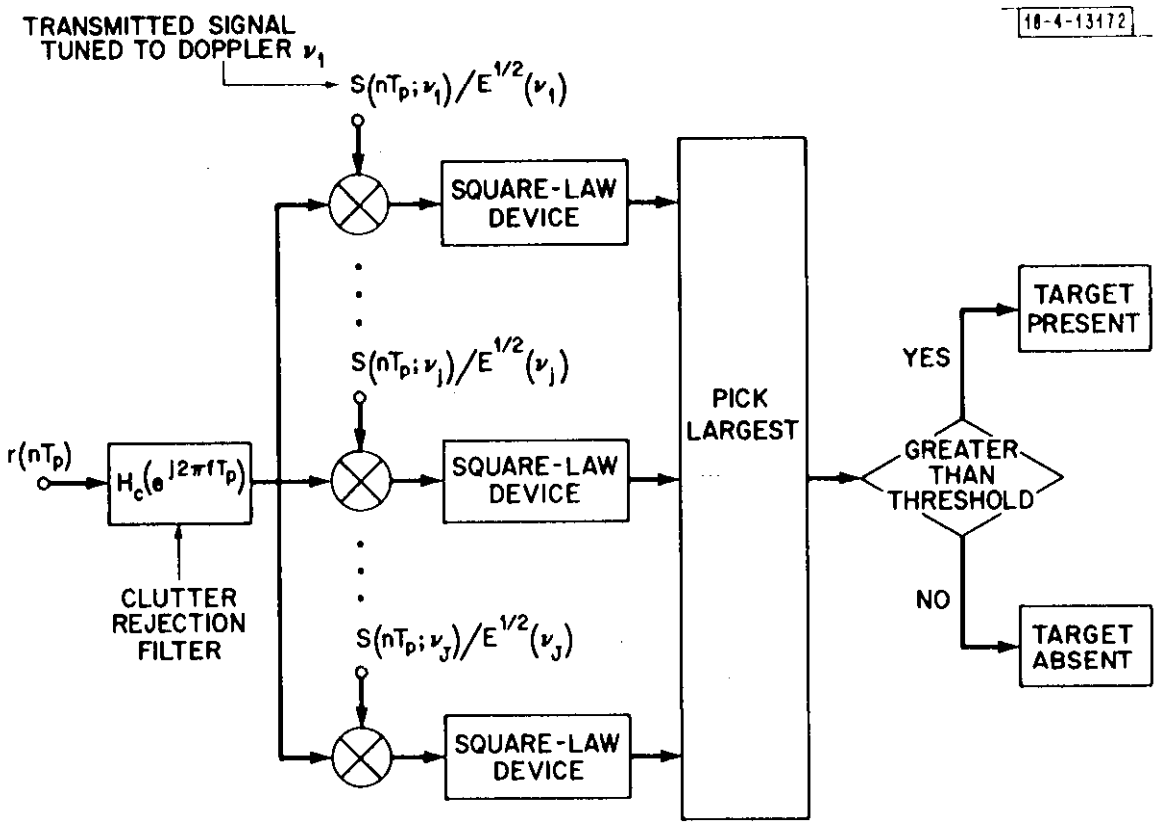

Fig. 4. Block diagram realization of optimum processor.

$$H_c(f) = \frac{1}{S_c(e^{j2\pi f T_p}) + 2N_o} \tag{62}$$

A typical clutter spectral density is illustrated in Fig. 5, as well as the resulting frequency characteristic of the clutter rejection filter. The sketch shows the effects of sampling in terms of aliasing the spectral density and the clutter filter characteristic. Furthermore the fact that the clutter filter inserts a notch at DC and at all multiples of the sampling frequency is reminiscent of the behavior of Classical MTI pulse cancellers. However, the derivation of the optimum MTI receiver provides the means whereby reasonable suboptimal approximations can be evaluated and compared. In the next section a design criterion that reflects the clutter rejection capabilities of a processor is defined and applied to the ARSR problem to evaluate the performance of classical MTI receivers as compared to the optimum processor.

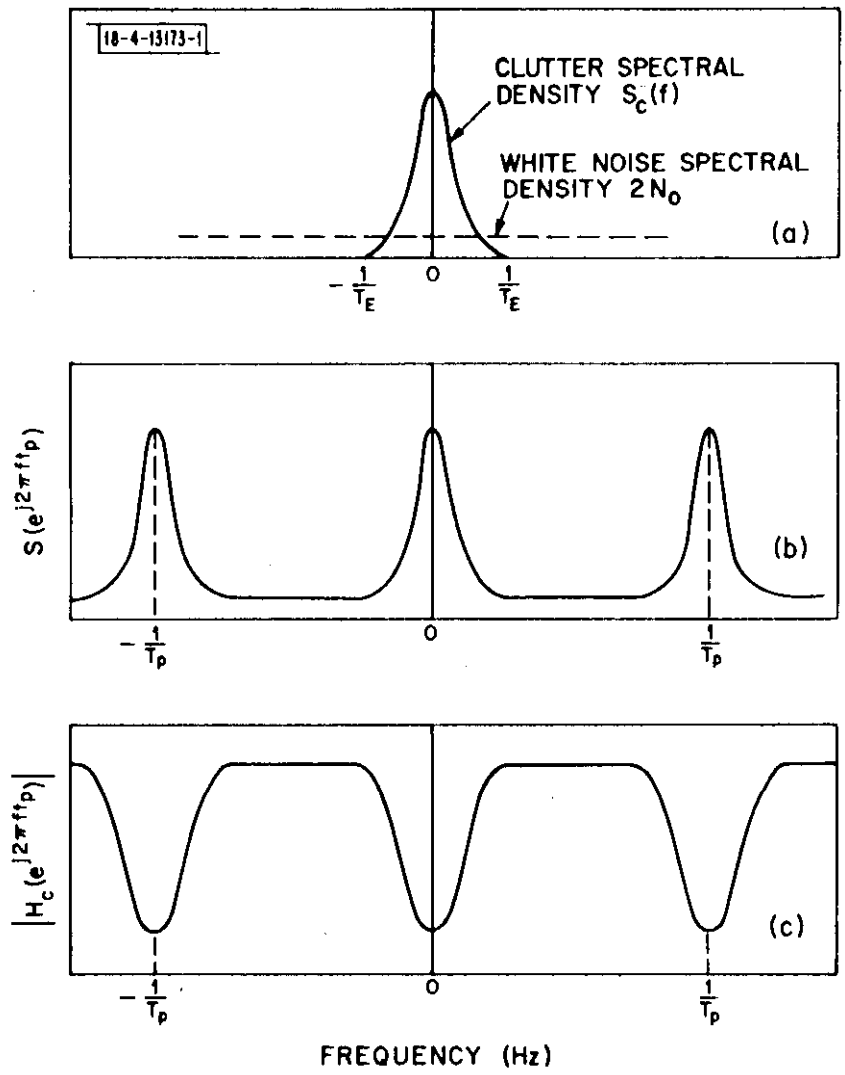

Fig. 5. Frequency characteristics of a typical clutter rejection filter.

IV. COMPARATIVE EVALUATION OF MTI PROCESSORS

The ideal criterion for evaluating the design of any detector is the trade-off between the probability of detection and the false alarm probability. In general these quantities are difficult to compute as they require precise knowledge of the statistics of the background clutter and noise. The performance measure adopted here, as in [4], [14] is mainly concerned with the ability of the receiver to detect targets in clutter. Since the optimum processor is a linear filter followed by a square-law envelope detector, it is reasonable to restrict the field of comparison to the class of linear filters. Then it is appropriate to measure the detection performance of any filter in the class by the signal-to-interference ratio (SIR) at the output of the filter. This quantity is defined to be

$$\rho \triangleq \frac{\text{instantaneous peak target output power}}{\text{average noise output power}} \quad . \tag{63}$$

When a target is present the received samples are

$$r(nT_p) = s(nT_p; \underline{\alpha}_o) + c(nT_p) + w(nT_p) \tag{64}$$

where $\underline{\alpha}_o = (\gamma_o, \tau_o, \nu_o)$ represents the true parameter values and

$$s(nT_p; \underline{\alpha}_o) = \gamma_o \, g(nT_p - \tau_o) \, e^{j2\pi\nu_o nT_p} \quad . \tag{65}$$

If $h(nT_p)$ is the impulse response of an arbitrary linear filter, the target output at each sampling time is

$$\xi_s(nT_p) = \sum_{k=-\infty}^{\infty} h(nT_p - kT_p) \, s(kT_p; \underline{\alpha}_o) \quad . \tag{66}$$

Therefore the instantaneous peak target power in $\xi_s(nT_p)$ can be expressed as

$$|\xi_s(nT_p)|^2 = \left|\frac{1}{2\pi j}\oint H(z)\, Z_s(z; \underline{\alpha}_o)\, z^{n-1}\, dz\right|^2 \tag{67}$$

where $H(z) = Z[h(nT_p)]$ and $Z_s(z; \underline{\alpha}_o) = Z[s(nT_p; \underline{\alpha}_o)]$. The noise samples at the output of the filter are

$$\xi_n(nT_p) = \sum_{k=-\infty}^{\infty} h(nT_p - kT_p)\,[Q(kT_p) + W(kT_p)] \tag{68}$$

and this output sequence has average noise power

$$|\xi_n(nT_p)|^2 = \frac{1}{2\pi j}\int H(z)\, H(\tfrac{1}{z})\,[S_c(z) + 2N_o]\, z^{-1}\, dz \quad . \tag{69}$$

Since the unit circle, $z = e^{j2\pi fT_p}$, is a legitimate contour of integration in the z-plane, the SIR at sample time τ is[5]

$$\rho(\tau) = \frac{\left|T_p \int_{-1/2\,T_p}^{1/2\,T_p} H(e^{j2\pi fT_p})\, Z_s(e^{j2\pi fT_p}; \underline{\alpha}_o)\,(e^{j2\pi fT_p})^{\tau/T_p}\, df\right|^2}{T_p \int_{-1/2\,T_p}^{1/2\,T_p} |H(e^{j2\pi fT_p})|^2\,[S_c(e^{j2\pi fT_p}) + 2N_o]\, df} \quad . \tag{70}$$

Since the Z-transform of (65) is [12]

$$Z_s(z; \underline{\alpha}_o) = \gamma_o\, G(e^{-j2\pi\nu_o T_p} z)\, z^{-\tau_o/T_p} \tag{71}$$

---

[5] τ and τ_o are assumed to be multiples of T_p

where $G(z) = Z[g(nT_p)]$, then (70) reduces to

$$\rho(\tau) = |\gamma_o|^2 T_p \frac{\left| \int_{-1/2T_p}^{1/2T_p} H(e^{j2\pi f T_p}) G(e^{j2\pi(f-\nu_o)T_p}) e^{j2\pi f(\tau-\tau_o)} df \right|^2}{\int_{-1/2T_p}^{1/2T_p} |H(e^{j2\pi f T_p})|^2 [S_c(e^{j2\pi f T_p}) + 2N_o] df} . \quad (72)$$

Using the Schwartz Inequality it can be shown that the SIR is maximum when

$$H(e^{j2\pi f T_p}) = \frac{1}{S_c(e^{j2\pi f T_p}) + 2N_o} \cdot \frac{G[e^{-j2\pi(f-\nu_o) T_p}]}{E^{\frac{1}{2}}(\nu_o)} . \quad (73)$$

This is precisely the cascade combination of the clutter rejection filter and the matched filter that is tuned to the true target doppler ν_o. Furthermore the maximum SIR is achieved only when the output of this filter is sampled at a time corresponding to the true target azimuth τ_o. Of course it is not possible to build such a filter because ν_o and τ_o are unknown a priori. However the maximum likelihood processor derived in Section III generates estimates τ, ν which in a well designed receiver are close to the true values τ_o, ν_o. Therefore the filter that maximizes the SIR can be visualized as being the filter in the matched filter bank that is most closely tuned to the true target doppler and sampled at a time τ that is closest to the true target azimuth. Therefore the maximum likelihood estimator, in addition to being an optimum filter in the decision theoretical sense,[6] is also optimum in the sense of

[6] Maximum probability of detection subject to a fixed false alarm probability.

maximizing the SIR. In the former case, the realization depended on the Gaussian noise assumption for the clutter statistics, but in the maximum SIR case, no Gaussian assumption is needed. Therefore the receiver has wide applicability in MTI problems.

The maximum SIR is found by using filter (73) in (72). This gives

$$\rho(\tau,\nu_o) = |\gamma_o|^2 T_p \frac{\left| \int_{-1/2\,T_p}^{1/2\,T_p} \frac{|G(e^{j2\pi(f-\nu_o)T_p})|}{S_c(e^{j2\pi fT_p}) + 2N_o} e^{j2\pi f(\tau-\tau_o)} df \right|^2}{\int_{-1/2\,T_p}^{1/2\,T_p} \frac{|G(e^{j2\pi(f-\nu_o)T_p})|^2}{S_c(e^{j2\pi fT_p}) + 2N_o} df} \qquad (74)$$

which when sampled at the correct time yields the maximum SIR

$$\rho_{opt}(\nu_o) = |\gamma_o|^2 T_p \int_{-1/2\,T_p}^{1/2\,T_p} \frac{|G(e^{j2\pi(f-\nu_o)T_p})|^2}{S_c(e^{j2\pi fT_p}) + 2N_o} df \quad . \qquad (75)$$

This result gives the ultimate performance capability of all linear MTI processors, digital or analog. Probably the reason this processor was not developed years ago, is due to the difficulty in realizing the matched filter bank at each range cell using analog hardware. With the advent of digital signal processing techniques, however, it is not at all unreasonable to consider a practical implementation of the optimum processor [13]. To determine whether or not this is a worthwhile project, it is necessary to compare its performance with well-known MTI receivers that may be considerably easier to implement. This can be done by specifying the MTI filter transfer

function and using (86), again assuming that the peak signal sample is taken. Then the SIR for suboptimal filters is

$$\rho_{sub}(\nu_o) = |\gamma_o|^2 T_p \frac{\left| \int_{-1/2T_p}^{1/2T_p} H(e^{j2\pi f T_p}) G[e^{j2\pi(f-\nu_o)T_p}]\, df \right|^2}{\int_{-1/2T_p}^{1/2T_p} |H(e^{j2\pi f T_p})|^2 [S_c(e^{j2\pi f T_p}) + 2N_o]\, df} \quad . \quad (76)$$

In order to evaluate (75) it is necessary to compute the Z-transform of the two-way antenna pattern and of its autocorrelation function. This task can often times be made simpler by relating the Z-transform to the Fourier Transform, since the latter is usually easier to compute. The desired relationship is deduced by representing the sampled data function $g(nT_p)$ as a continuous waveform using

$$\hat{g}(t) = g(t) \sum_{n=-\infty}^{\infty} \delta(t - nT_p) \quad (77)$$

where $\delta(t)$ is an ideal sampling pulse, the Dirac Delta function. Then if $L[\hat{g}(t)]$ denotes the Laplace Transform of $\hat{g}(t)$, then it is a fact [15] that

$$Z[g(nT_p)] = L[\hat{g}(t)]_s = \frac{1}{T_p} \ln z \quad . \quad (78)$$

Therefore when g(t) is a well-behaved function

$$G(e^{j2\pi f T_p}) = Z[g(nT_p)]_z = e^{j2\pi f T_p}$$

$$= L[\hat{g}(t)]_s = j2\pi f = F[\hat{g}(t)] \quad (79)$$

where $F[\hat{g}(t)]$ is the Fourier Transform of $\hat{g}(t)$. From (91)

$$F[\hat{g}(t)] = F[g(t)] * \sum_{n=-\infty}^{\infty} \delta(f - \frac{n}{T_p})$$

$$= \frac{1}{T_p} \sum_{n=-\infty}^{\infty} F_g(f - \frac{n}{T_p}) \qquad (80)$$

where $F_g(t) = F[g(t)]$ and "*" denotes convolution. Therefore

$$G[e^{j2\pi(f - \nu_o)T_p}] = \frac{1}{T_p} \sum_{n=-\infty}^{\infty} F_g(f - \nu_o - \frac{n}{T_p}) \quad . \qquad (81)$$

In order to make use of (81) in (75) it is necessary to use the term in the sum that lies in the $(-1/2\,T_p,\ 1/2\,T_p)$ frequency interval. This can be made clear by noting that $F_g(t)$ is narrowband about DC, and then writing

$$\nu_o = \frac{m_o}{T_p} + \Delta\nu_o \qquad (82)$$

where $|\Delta\nu_o| \leq 1/2\,T_p$

$$G[e^{j2\pi(f - \nu_o)}] = \frac{1}{T_p} F_g(f - \Delta\nu_o) \qquad |f| \leq 1/2\,T_p \quad . \qquad (83)$$

Since the spectral density of a discrete time random process is the Z-transform of the sampled correlation function, then

$$S(e^{j2\pi fT_p}) = Z[R(nT_p)]_{z = e^{j2\pi fT_p}}$$

$$= F[R(t)] * \frac{1}{T_p} \sum_{n=-\infty}^{\infty} \delta(f - \frac{n}{T_p}) \quad . \tag{84}$$

To evaluate (73) and (76) only those frequency terms out to $\pm 1/2\,T_p$ are of interest, therefore for $|f| \leq 1/2\,T_p$

$$S(e^{j2\pi fT_p}) = \frac{1}{T_p} F[R(t)] \quad . \tag{85}$$

R(t) is the correlation function of the continuous time clutter process and in this case is given by

$$R_c(t) = \frac{\sigma^2}{T_p} R_g(t) \tag{86}$$

where

$$R_g(t) = \int_{-\infty}^{\infty} g(\sigma)\ g(\sigma + t)\ d\sigma \quad . \tag{87}$$

Since $F[R_g(t)] = |F_g(f)|^2$, then using (85) the spectral density of the clutter process is

$$S_c(e^{j2\pi fT_p}) = \frac{1}{T_p}\left[\frac{\sigma^2}{T_s} |F_g(f)|^2\right], \qquad |f| \leq 1/2\,T_p \quad . \tag{88}$$

Using (83) and (88) in (75) and (76) the final expressions for the signal-to-interference ratios are

$$\rho_{opt}(\nu_o) = |\gamma_o|^2 \int_{-1/2T_p}^{1/2T_p} \frac{|F_g(-\Delta\nu_o)|^2}{\frac{\sigma^2}{T_s}|F_g(f)|^2 + 2N_o T_p}\, df \tag{89}$$

$$\rho_{sub}(\nu_o) = |\gamma_o|^2 \frac{\left| \int_{-1/2T_p}^{1/2T_p} H(e^{j2\pi f T_p})\, F_g(f-\Delta\nu_o)\, df \right|^2}{\int_{-1/2T_p}^{1/2T_p} |H(e^{j2\pi f T_p})|^2 \left[\frac{\sigma^2}{T_s}|F_g(f)|^2 + 2N_o T_p\right] df} \tag{90}$$

where $\nu_o = \frac{m_o}{T_p} + \Delta\nu_o$ with $|\Delta\nu_o| \leq 1/2T_p$. (91)

Therefore to make a performance calculation it is necessary to:

1. Specify the two-way antenna voltage gain pattern as a function of azimuth (i.e., $G^2(\theta)$, $|\theta| \leq \pi$).
2. Compute the time function $g(t) = G^2(\omega_s t)$, where ω_s is the scan rate of the radar (rad/sec.).
3. Compute the Fourier Transform

$$F_g(f) = \int_{-T_s/2}^{T_s/2} g(t)\, e^{-j2\pi ft}\, dt \quad \omega_s T_s = 2\pi \ . \tag{92}$$

4. Specify the sampled-data impulse response for the suboptimal filter, $h(nT_p)$ and compute its Z-transform, $H(z)$, which is in turn evaluated at $z = e^{j2\pi f t_p}$.

In the paragraphs that follow, these steps will be applied to a $\sin x/x$

antenna pattern and several MTI filters that are representative of practical implementations.

sin x/x Antenna Pattern

The sin x/x antenna pattern is extremely convenient to manipulate analytically and is fairly representative of those encountered in practice. It will be adopted as the basic pattern for the remainder of this study. This means that

$$G(\theta) = \frac{\sin(\theta/\Delta\theta)}{(\theta/\Delta\theta)} \tag{93}$$

where $\Delta\theta$ is related to the antenna half-beamwidth. Then

$$g(t) = \left[\frac{\sin(\omega_s t/\Delta\theta)}{(\omega_s t/\Delta\theta)}\right]^2 \tag{94}$$

It is easily shown that the Fourier Transform of g(t) in (108) is

$$F_g(f) = \begin{cases} \frac{\Delta\theta}{\omega_s}\left[1 - \frac{\Delta\theta}{\omega_s}|f|\right] & |f| \leq \frac{\omega_s}{\Delta\theta} \\ 0 & \text{otherwise} \end{cases} . \tag{95}$$

Let T_E denote the time it takes the antenna to scan through $\Delta\theta$ radians so that

$$\omega_s T_E = \Delta\theta \quad . \tag{96}$$

Since all of the effective target reports occur only as the main beam of the antenna is on the aircraft, it is clear that T_E measures the effective time on target. Substituting (96) into (93) and the result into (88) gives for the clutter spectral density

$$S_c(e^{j2\pi f T_p}) = \begin{cases} \sigma^2 \dfrac{T_E^2}{T_s T_p} [1 - T_E|f|^2] & |f| \leq 1/T_E \\ 0 & 1/T_E < |f| \leq 1/T_p \end{cases} . \quad (97)$$

Since $C(nT_p)$ represents a sample of the clutter as seen by the two-way antenna voltage pattern, $|C(nT_p)|^2$ represents the clutter energy per sample. From sampled-data theory it is known that the average energy per sample is

$$\overline{|C(nT_p)|^2} = T_p \int_{-1/2T_p}^{1/2T_p} S_c(e^{j2\pi f T_p}) \, df . \quad (98)$$

Using (97) in (98) it follows that the average clutter power at the receiver input due to clutter in a 360° range resolution ring is

$$P_c = \frac{2}{3} \cdot \sigma^2 \frac{T_E}{T_s} . \quad (99)$$

Since $T_s/T_E = 2\pi/\Delta\theta$ represents the number of azimuth cells, each one beamwidth in extent, and since the factor 2/3 arises from the assumed $\sin x/x$ beam pattern, then it is clear that σ^2 represents the average clutter power that would be received by an omnidirectional antenna due to scatters throughout the 360° range resolution ring. It is appropriate to define another parameter

$$\sigma_c^2 = \sigma^2/(T_s/T_E) \quad (100)$$

as this represents the average clutter power inherent in the scatterers located in one range-azimuth cell as defined by the antenna beamwidth $\Delta\theta$. Since this is an easier quantity to compute analytically, it will be used in future

calculations. Therefore (97) becomes

$$S_c(e^{j2\pi f T_p}) = \begin{cases} \sigma_c^2 \frac{T_E}{T_p} [1 - T_E|f|]^2 & |f| \leq 1/T_E \\ 0 & 1/T_E < |f| \leq 1/2\,T_p \end{cases} . \quad (101)$$

Since $F_g(f)$ is also needed in the evaluation of the optimum receiver, then in terms of T_E (95) becomes

$$F_g(f) \begin{cases} T_E[1 - T_E|f|] & |f| \leq 1/T_E \\ 0 & \text{otherwise} \end{cases} . \quad (102)$$

Optimum MTI Performance

Since the structure of the maximum likelihood receiver depends only on the antenna pattern, (102) can be used with (89) to evaluate its performance in terms of the SIR performance index. Some typical results based on the ARSR system parameters, [16] are shown in Fig. 6 for various values of σ_c^2. Since the PRF is 360 pps the SIR performance curve is periodic with doppler period 360 Hz. It is also symmetric about DC a result that holds in general since the two-way voltage gain antenna pattern is real. The target and clutter power returns are calculated on the basis of an aircraft located in a range ring at 100 nautical miles. For targets at closer ranges the performance will be significantly improved because target power follows an R^{-4} law while the clutter depends on R^{-3}. Therefore the results are conservative for the near-in ground clutter which has been most troublesome so far as the ARSR is concerned.

MTI Pulse Cancellers

To appreciate the significance of the previous results it is necessary to

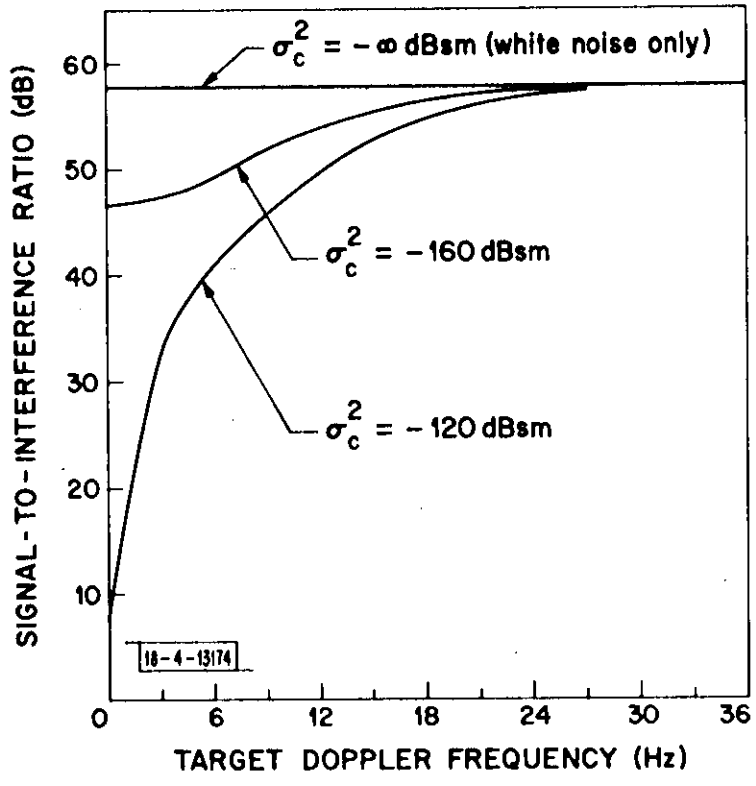

Fig. 6. Signal-to-interference ratio of the optimum processor.

compare the performance with MTI techniques that are commonly used in practice. Classical MTI methods are simply approximations to the clutter rejection filter; no matched filtering is used. The simplest pulse canceller subtracts successive radar returns. Since a stationary object would produce identical returns in the same range cell, the clutter would be cancelled and only moving target returns would remain. The problem is that a scanning antenna renders all fixed target returns nonstationary, hence much of the ground clutter must pass through this type of filter. This deficiency in the two pulse canceller can be made quantitative by defining the appropriate sampled-data impulse response and then apply (90) to compute the SIR. To specify the filter it is noted that if $r(nT_p)$ denotes the radar samples corresponding to a particular range, then the output of the pulse canceller is

$$\xi(nT_p) = r(nT_p) - r[(n-1)\,T_p] \quad . \tag{103}$$

This corresponds to a sampled-data filter whose impulse response is

$$\begin{aligned} h(0) &= 1 \\ h(T_p) &= -1 \\ h(nT_p) &= 0 \qquad n \neq 0,\ n \neq 1 \quad . \end{aligned} \tag{104}$$

The transfer function is therefore

$$H(z) = \frac{z-1}{z} \tag{105}$$

and along $|z| = 1$

$$H(e^{j2\pi fT_p}) = 1 - e^{-j2\pi fT_p} \quad . \tag{106}$$

The familiar form for the magnitude function is

$$|H(e^{j2\pi fT_p})| = 2\left|\sin \pi f T_p\right| \quad . \tag{107}$$

Using (101) and (102) in (90), the SIR performance curve can be computed. It is plotted in Fig. 7 for a typical clutter power level and compared with the optimum SIR possible. One reason the two-pulse canceller performs so poorly in comparison to the optimum is due to the fact that the actual clutter spectral density is spread about DC as a result of the antenna motion. Had the clutter returns been truly stationary this filter should perform quite well since it locates a null at DC.

Higher Order Pulse Cancellers

In order to further eliminate the higher frequency components in the clutter returns, higher order pulse cancellers are used. With these a broader rejection notch at DC should result in improved clutter rejection. An upper bound on the SIR performance of this class of filters can be found by designing an ideal notch to eliminate all of the clutter. Mathematically this requires that

$$H(e^{j2\pi fT_p}) = \begin{cases} 1 & |f| \leq 1/T_E \\ 0 & 1/T_E < |f| \leq 1/T_p \end{cases} \tag{108}$$

which corresponds to the sampled-data impulse response

$$h(nT_p) = \frac{1}{n} \sin\left(\frac{2\pi n T_p}{T_E}\right) \quad n = 0, \pm 1, \pm 2, \ldots \tag{109}$$

Using (90) the SIR performance of (108) can be computed for the sin x/x

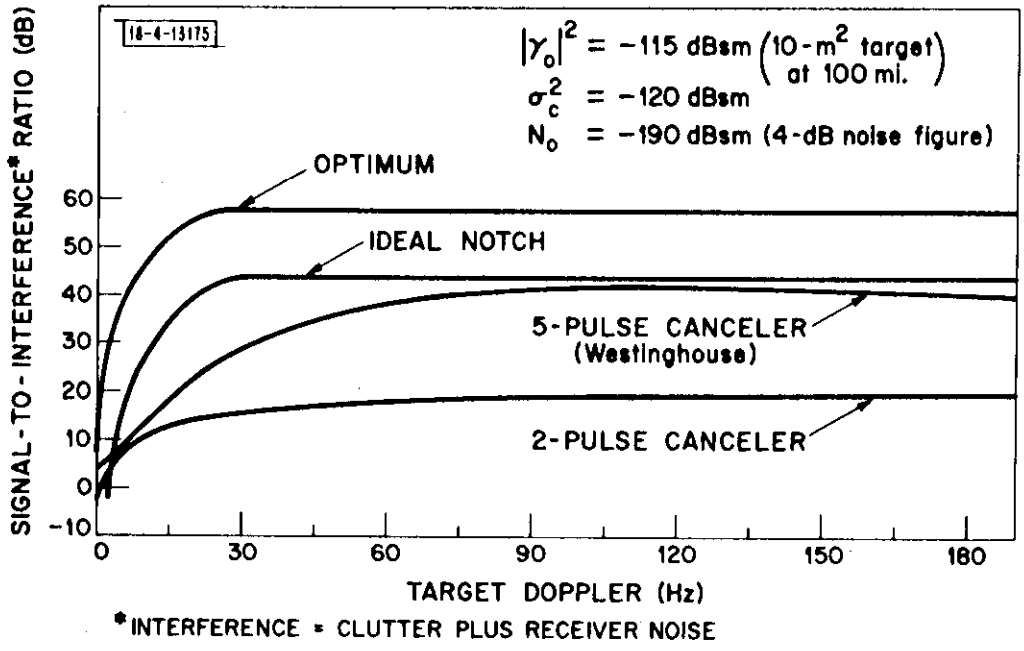

Fig. 7. Signal-to-interference ratios of well known MTI filters.

antenna pattern. The results are shown in Fig. 7 in comparison with the optimum filter and the two pulse canceller. It is clear that although the notch filter is considerably less than optimum significant improvements in performance over the two-pulse canceller is obtained.

Digital MTI radars have recently been constructed which use higher order pulse cancellers to approximate the ideal notch filter [6]. Using the formula for the suboptimum SIR, the performance of the proposed filter can be calculated. The filter of interest is a five-pulse canceller that has a frequency response that is zero at DC and a least squares fit to the ideal notch elsewhere. In this case the sampled-data impulse response is

$$\begin{aligned} h(-2) &= h(2) = a_2 \\ h(-1) &= h(1) = a_1 \\ h(0) &= a_o \\ h(n) &= 0 \qquad |n| > 2 \quad . \end{aligned} \tag{110}$$

In other words, if $r(kT_p)$ is the received sequence then the filter output is

$$\xi(kT_p) = a_2\, r(k+2) + a_1\, r(k+1) + a_o\, r(k) + a_1\, r(k-1) + a_2\, r(k-2). \tag{111}$$

The z-transform of the impulse response is

$$H(z) = a_2\, z^2 + a_1\, z + a_o + a_1\, z^{-1} + a_2\, z^{-2} \tag{112}$$

and the function needed in the SIR evaluation is

$$H(e^{j2\pi fT_p}) = a_o + 2a_1 \cos 2\pi fT_p + 2a_2 \cos 4\pi fT_p \quad . \tag{113}$$

Although the filter is non-causal since it requires future inputs to process a present value, it can easily be implemented by allowing $2T_p$ sec. of delay between input and output. The coefficients a_o, a_1, a_2 are chosen so that (113) is a minimum-mean-squared-error fit to the ideal notch (108) subject to the constraint H (f = 0) = 0. Equation (90) is used to obtain the suboptimum SIR for this filter. Although the ideal notch and the more practical pulse cancellers provide some SIR improvement there is at least a 10-dB loss relative to the performance of the optimum filter. The reason for this is due to the enhanced receiver noise rejection properties of the matched filter bank of the optimum receiver. If the ideal notch filter is used in cascade with the matched filter bank, then essentially optimum SIR performance is obtained.

V. AZIMUTH ESTIMATION ACCURACY

So far the analysis has been concerned with the ability of an MTI receiver to estimate target doppler. Another parameter obtainable from the radar sensor is the aircraft azimuth. In the MTI context this corresponds to estimating τ, the center of the two-way antenna pattern. It is well known [5] that the maximum likelihood estimator generates minimum variance time of arrival estimates when the SNR is large. In the present context this means that

$$\overline{(\hat{\tau} - \tau_o)^2} = \left(\frac{|\gamma_o|^2 E}{2N_o} \cdot \overline{\omega^2} \right)^{-1} \tag{114}$$

where

$$E = \frac{1}{T_p} \int_{-1/2\,T_p}^{1/2\,T_p} |F_g(f)|^2 \, df \tag{115a}$$

$$\overline{\omega^2} = \frac{4\pi^2 \int_{-\infty}^{\infty} f^2 |F_g(f)|^2 \, df}{\int_{-\infty}^{\infty} |F_g(f)|^2 \, df} \tag{115b}$$

The term $|\gamma_o|^2 E/N_o$ represents the clutter-free SNR at the output of the MTI processor due to match filtering all of the signal pulses received in one sweep past the aircraft, while ω^2 represents the Gabor bandwidth of the two-way antenna modulation. Equation (102) defines $F_g(f)$ for the $\sin x/x$ antenna pattern which can be used in (115) to yield

$$\overline{\omega^2} = 4\pi^2/10\,T_E^2 \quad . \tag{116}$$

Using the fact that when a detection is made in the m^{th} range ring, the azimuth is given by

$$\varphi = \omega_s(\tau + m\Delta T/2) \tag{117}$$

then

$$\overline{(\hat{\varphi} - \varphi_o)^2} = \omega_s^2\,\overline{(\hat{\tau} - \tau_o)^2} \tag{118}$$

Using the fact that $\omega_s T_E = \Delta\theta$ where $\Delta\theta$ is the defined beamwidth of the two-way antenna pattern, then the mean-squared azimuth error is

$$\overline{(\hat{\varphi} - \varphi_o)^2} = \frac{N_o}{|\gamma_o|^2 E} \cdot \frac{5}{\pi^2} \cdot (\Delta\theta)^2 \tag{119}$$

Signal processing therefore leads to azimuth estimates more accurate than a beamwidth when

$$\frac{|\gamma_o|^2 E}{N_o} \cong \frac{5}{\pi^2} \tag{120}$$

which corresponds to -3 dB received SNR. On the other hand when the received SNR is greater than 17 dB 10:1 improvements in the standard deviation of the azimuth estimate can be obtained.

These improvements do not come for free however, since the ultimate accuracy is tied to how many points are allowed to pass before another DFT is taken. It will be necessary to perform a trade-off between the desired

azimuth accuracy and the number of points the data window is allowed to shift before the next DFT is taken. The point is, that considerable improvements are theoretically and practically possible; it remains to determine the expense involved in achieving these gains.

VI. ALL-WEATHER MTI

Although the previous discussion has been concerned with the rejection of ground clutter, the results are actually applicable to the problem of eliminating clutter due to any source so long as its spectral density does not extend beyond the rejection band of the notch filter. Therefore it is expected that the detector should perform well in many adverse environmental conditions except those in which the overall mass of the clutter "cloud" has a significant radial velocity. Since the scattering centers in a weather cloud will be in motion relative to one another, the spectral density of the clutter returns will extend over a larger frequency interval than that of the ground clutter background. Since the doppler filters are designed on the basis of this latter quantity, the enhanced velocity resolution will subdivide the power in the weather cloud and its overall effect on target detection will be reduced. In the time domain this effect is explained by noting that the motion of the scatterers causes the weather clutter to decorrelate faster than the ground clutter which means that integration of all of the pulses in a beamwidth will lead to some improvement in target detection. Unfortunately it is likely that the power levels in each of these filters will exceed the receiver noise threshold setting resulting in false alarms in the low velocity filters. However since weather clutter will probably cause false alarms in several adjacent low velocity filters it can be recognized as clutter and disregarded. Although this is a simple and attractive scheme for eliminating false alarms, the detection probability degrades to zero and clearly an alternate choice is sought. Rather than just recognize and eliminate false alarms, it is necessary for the receiver to raise the detection threshold in those velocity cells that are covered by the clutter cloud. Adaptive

algorithms have been derived [18] that estimate the average clutter power and use this value to reset the detection threshold. In this case, the estimate would be derived by averaging over the clutter returns in a range ring which had been gathered scan-to-scan. The optimality properties of this algorithm are based on the assumption that except for an amplitude scale factor the clutter correlation function is known. This is an unrealistic assumption in the present context since the velocity of the weather cloud and the width of the associated spectral density will vary on an hour-to-hour basis. However, a suboptimal algorithm can be deduced by further subdividing the clutter space into the DFT velocity cells. Since the clutter spectral density is unlikely to change significantly over the width of one velocity cell, the clutter can be considered to be white noise of unknown average power. This is easily estimated by the scan-to-scan averaging of the power measured in the velocity cell. The detection threshold can then be set for the particular velocity cell of interest by combining the estimated clutter power level with that of the receiver noise process.

The above algorithms may well prove to be of considerable utility in the struggle to diminish the effects of weather clutter, but it will be necessary to build an experimental system before final judgment can be passed. Since the preceding discussion is based on intuitive considerations, it is of interest to determine whether or not optimal weather processors can be derived and what their role might be in a practical deployment of the MTI receiver. The next few paragraphs document the first order study of the latter problem.

In the background of ground and weather clutter, the clutter process is more precisely written as

$$C(nT_p) = C_g(nT_p) + C_w(nT_p) \quad . \tag{121}$$

Formerly $C_g(nT_p)$ referred to the ground clutter samples, but it will now be taken to denote any clutter due to ground scattering or weather returns that induce no doppler shift. The new term $C_w(nT_p)$ refers to the clutter samples from a weather cloud that is moving at some non-zero radial velocity. The optimum receiver synthesized in the preceding sections is directly applicable to the weather processing problem, except now the clutter spectral density is

$$S_c(f) = S_g(f) + S_w(f - f_w) \tag{122}$$

where f_w is used to indicate the average doppler shift induced by the moving cloud. It will be assumed that $S_g(f)$ and $S_w(f - f_w)$ are non-overlapping spectral densities, so that

$$S_g(f) \cdot S_w(f - f_w) = 0 \quad . \tag{123}$$

From the analysis of the preceding sections the clutter processing is done by the clutter rejection filter having transfer function given by

---

For convenience the notation $S_c(f)$ is used in place of $S_c(e^{j2\pi fT_p})$.

$$H_c(f) = \frac{1}{S_c(f) + 2N_o}$$

$$= \frac{1}{S_g(f) + S_w(f - f_w) + 2N_o}$$

$$= \frac{1}{S_g(f) + 2N_o} \left[\frac{S_g(f) + 2N_o}{S_g(f) + S_w(f - f_w) + 2N_o} \right]$$

$$= \frac{1}{S_g(f) + 2N_o} \cdot \left[1 - \frac{S_w(f - f_w)}{S_g(f) + S_w(f - f_w) + 2N_o} \right] . \qquad (124)$$

Using the assumption in (123) in the last equation results in the following final form for the ground plus weather clutter filter

$$H_c(f) = \frac{1}{S_g(f) + 2N_o} \cdot \left[1 - \frac{S_w(f - f_w)}{S_w(f - f_w) + 2N_o} \right] . \qquad (125)$$

Therefore the weather clutter is processed by a separate filter that is an adjunct to the ground clutter notch filter discussed in the previous sections. It was shown that the optimum clutter filter was well approximated by a notch filter with an elimination band about DC to reject all signals due to both slow targets and ground clutter returns. Therefore to a good approximation the output of the ground clutter filter can be assumed to be made up of signals due to faster moving targets, receiver white noise and weather clutter returns. In other words the output of the ground clutter filter can be assumed to be

$$r(nT_p) = \gamma_o\, g(nT_p - \tau_o)\, e^{j2\pi\nu_o nT_p} + C_w(nT_p) + W(nT_p) \qquad (126)$$

when a moving target is present and it is

$$r(nT_p) = C_w(nT_p) + W(nT_p) \qquad (127)$$

when the target is absent. In the latter case, the filter having the transfer function

$$\frac{S_w(f - f_w)}{S_w(f - f_w) + 2N_o} \qquad (128)$$

generates the minimum-mean-squared error (MMSE) estimate of the weather clutter waveform. Therefore the processor in (125) has the following interpretation: First eliminate ground clutter returns using the notch filter; then process the remaining weather clutter and white noise output to generate a MMSE estimate of the weather clutter signal, referred to as $\hat{C}_w(nT_p)$. This is subtracted from the composite signal in (127) to yield

$$r(nT_p) - \hat{C}_w(nT_p) = [C_w(nT_p) - \hat{C}_w(nT_p)] + W(nT_p) \qquad (129)$$

which shows how the weather clutter filter tries to eliminate the clutter waveform.

If the weather clutter spectral density is known then the filter in (124) can be synthesized directly without recourse to the MMSE interpretation. However, this is precisely the problem with weather clutter; it is a random process whose gross statistics change significantly from weather cloud to weather

cloud. It is therefore essential that some adaptivity be built into the receiver to track the gross changes in statistics of the weather clutter process. The MMSE filter realization provides the basic structure for deriving the desired adaptivity. Since the key element in the weather clutter processor is a linear filter that generates the MMSE estimates of the weather clutter waveform when no target is present, it can be replaced by a tapped delay line whose taps are up-dated recursively using, for example, the stochastic approximation algorithm described in [19]. Since any weather cloud can reasonably be assumed to be a quasi-stationary process in the sense that its statistics do not change significantly over many scans of the radar, many independent sample functions are available which can be used to adapt the filter to give near optimum MMSE estimates of the weather clutter waveform. The computational problem can be simplified somewhat by postulating a weather clutter spectral density whose form is generally known except for a center frequency, a magnitude scale factor, and a spectral spread factor. The received sample functions can then be used to adaptively estimate these three parameters. Once convergence has been obtained the matched filter bank normalization factor in (56) and (A-13) can be computed. This will insure that a constant false alarm rate (CFAR) receiver will result.

This area of research is highly speculative since the ideas, originally suggested in [9], have never been applied to a practical problem. However it does show what must be done to perform optimum weather and ground clutter processing and it may very well prove useful in the MTI processor of the future.

VII. INTRODUCTION TO PART II

If the doppler frequency caused by the maximum target velocity is less than $1/2\,T_p$ in magnitude then the digital MTI processor described in the preceeding paragraphs comes very close to achieving optimum performance and can be implemented using current digital technology. If on the other hand, the induced doppler shifts are larger than $1/2\,T_p$, as is the case with the ARSR, then the broad clutter notch at DC effectively folds over to eliminate from detection targets whose dopplers correspond to some multiple of $1/T_p$. In such a case the performance of the filter is quite unsatisfactory. The reason for the aliasing is of course due to the uniform sampling pattern. It is well known in classical MTI that staggering the PRF, which means non-uniform sampling, eliminates the so-called blind velocities so that targets moving with dopplers at n/T_p can once again be detected [17]. Although this technique has been used for many years in practice no theoretical analysis of the phenomenon has been presented. As a result the classical investigators failed to realize that non-uniform sampling not only enhances target detection capability but also permits the unambiguous resolution of target velocity. In Part II of this paper it is shown that designing the staggered sampling pattern is equivalent to shaping the ambiguity function of a pulse train. Hence staggering the sampling pattern reduces to a signal design problem which in conjunction with the optimum processor described in this paper leads to an MTI receiver that has never before been proposed for moving target indication It is the first time that this author has seen the maximum likelihood method lead to a receiver that some intuitive engineer had not discovered a decade earlier.

APPENDIX

In Section III the likelihood function for the optimum MTI receiver was derived in terms of whitened versions of the transmitted and received signal sequence. Since this is an inconvenient receiver structure to implement alternate realizations are sought. It will now be shown how the likelihood equation can be manipulated to suggest the clutter filter, matched filter realization. The following notation is needed:

$$R_w(z) = Z[r_w(nT_p)] \tag{A-1a}$$

$$S_w(z; \underline{\alpha}) = Z[S_w(nT_p; \underline{\alpha})] \tag{A-1b}$$

$$\hat{S}_w(z; \underline{\alpha}) = Z[S^*_w(nT_p; \underline{\alpha})] \quad . \tag{A-1c}$$

Using the complex convolution theorem for sampled-data sequences [11], the term in the numerator of (56) can be written as

$$\sum_{n=-\infty}^{\infty} r_w(nT_p)\, S^*_w(nT_p; \underline{\alpha}) = \frac{1}{2\pi j} \oint R_w(z)\, \hat{S}_w\left(\frac{1}{z}, \underline{\alpha}\right) z^{-1}\, dz \tag{A-2}$$

where the integral is to be evaluated along some suitably defined path in the z-plane. The denominator in (56) can be considered a normalization factor

$$E(\underline{\alpha}) \triangleq \sum_{n=-\infty}^{\infty} |S^*_w(nT_p; \underline{\alpha})|^2$$

$$= \frac{1}{2\pi j} \oint S_w(z; \underline{\alpha})\, \hat{S}_w\left(\frac{1}{z}; \underline{\alpha}\right) z^{-1}\, dz \quad . \tag{A-3}$$

For the input signals, the following notation is needed:

$$R(z) = Z[r(nT_p)] \tag{A-4a}$$

$$S(z; \underline{\alpha}) = Z[S(nT_p; \underline{\alpha})] \tag{A-4b}$$

$$S(z; \underline{\alpha}) = Z[S^*(nT_p; \underline{\alpha})] \quad . \tag{A-4c}$$

These functions are related to those in (A-1) according to

$$R_w(z) = H_w(z)\, R(z) \tag{A-5a}$$

$$S_w(z; \underline{\alpha}) = H_w(z)\, S(z; \underline{\alpha}) \tag{A-5b}$$

$$\hat{S}_w(z; \underline{\alpha}) = H_w(z)\, \hat{S}(z; \underline{\alpha}) \quad . \tag{A-5c}$$

The last expression uses the fact that the impulse response of the whitening filter is real. Then (A-2) becomes

$$\sum_{n=-\infty}^{\infty} \mathbf{r}_w(nT_p)\, S_w^*(nT_p; \underline{\alpha}) = \frac{1}{2\pi j} \oint \left[H_w(z)\, R(z)\right] \left[H_w(\tfrac{1}{z})\, \hat{S}(\tfrac{1}{z}; \underline{\alpha})\right] z^{-1}\, dz$$

$$= \frac{1}{2\pi j} \oint \left[H_w(z)\, H_w(\tfrac{1}{z})\, R(z)\right] \hat{S}(\tfrac{1}{z}; \underline{\alpha})\, z^{-1}\, dz$$

$$= \sum_{n=-\infty}^{\infty} \mathbf{x}(nT_p)\, S^*(nT_p; \underline{\alpha}) \tag{A-6}$$

where

$$x(nT_p) = Z^{-1}\left[H_w(z)\, H_w(\tfrac{1}{z})\, R(z)\right] \quad . \tag{A-7}$$

Similarly (A-3) becomes

$$E(\underline{\alpha}) = \frac{1}{2\pi j} \oint \left[H_w(z)\, H_w(\tfrac{1}{z})\, S(z; \underline{\alpha})\right] \hat{S}(\tfrac{1}{z}; \underline{\alpha})\, z^{-1}\, dz$$

$$= \sum_{n=-\infty}^{\infty} y(nT_p)\, S^*(nT_p; \underline{\alpha}) \tag{A-8}$$

where

$$y(nT_p) = Z^{-1}\left[H_w(z)\, H_w(\tfrac{1}{z})\, S(z; \underline{\alpha})\right] \quad . \tag{A-9}$$

For the problem at hand $\underline{\alpha} = (\nu, \tau)$ and

$$S(nT_p; \underline{\alpha}) = g(nT_p - \tau)\, e^{j2\pi\nu nT_p} \quad . \tag{A-10}$$

Since $g(nT_p)$ is real,

$$S^*(nT_p; \underline{\alpha}) = g(nT_p - \tau)\, e^{-j2\pi\nu nT_p} \tag{A-11}$$

hence[8]

$$S(z; \underline{\alpha}) = e^{j2\pi\nu\tau}\, z^{-\tau/T_p}\, G(e^{-j2\pi\nu T_p} z) \tag{A-12a}$$

$$S(z; \underline{\alpha}) = e^{-j2\pi\nu\tau}\, z^{-\tau/T_p}\, G(e^{j2\pi\nu T_p} z) \tag{A-12b}$$

where $G(z) = Z[g(nT_p)]$. Using (66) and (A-12) in (A-8) the denominator of the test statistic becomes

[8] τ is assumed to be a multiple of T_p.

$$E(\nu,\ \tau) = \frac{1}{2\pi j} \oint H_c(z)\ G(z\ e^{j2\pi\nu T_p})\ G(\frac{1}{z}\ e^{j2\pi\nu T_p})\ z^{-1}\ dz$$

$$= E(\nu) \quad . \tag{A-13}$$

Equation (A-13) shows that the energy normalization factor depends only in the doppler frequency under test.

ACKNOWLEDGMENTS

The study documented in this report is the result of considerable interaction and cooperation of members of the Air Traffic Control Division and the Lincoln Laboratory Radar Techniques Program. The author would especially like to express his appreciation to P. R. Drouilhet who motivated the study, and to T. Bially, L. Cartledge, T. J. Goblick, E. M. Hofstetter and E. J. Kelly who contributed to the author's understanding of MTI radar. Collaboration with R. D. Yates led to the basic formulation of the MTI detection problem in terms of the sampled-data processing of data in range rings and J. R. Johnson provided a key analytical manipulation that led to the spectrum of the staggered PRF transmitted signal. Finally, the author would like to thank A. F. Pensa who wrote the computer programs that generated the SIR performance curves.

REFERENCES

[1] M. I. Skolnik, Introduction to Radar Systems (McGraw-Hill Book Co., New York, 1962), Chapter 4.

[2] B. D. Steinberg, "Target Clutter and Noise Spectra," Part VI, Chapter I, in Modern Radar (B. J. Berkowitz, John Wiley and Sons, Inc., New York, 1965).

[3] P. Bradsell, "Moving Target Indication: A Survey of Developments since 1948," Chapter 9 in Radar Techniques for Detection Tracking and Navigation by W. T. Blackband, (Gordon and Breach Science Publishers, New York, 1966).

[4] E. M. Hofstetter, C. J. Weinstein and C. E. Muehe, "A Theory of Multiple Antenna AMTI Radar," Technical Note 1971-21, Lincoln Laboratory, M.I.T. (8 April 1971).

[5] E. J. Kelly, I. S. Reed and W. L. Root, "The Detection of Radar Echoes in Noise. II," J. Soc. Indust. Appl. Math., Vol. 8, No. 3 September 1960, pp. 495.

[6] R. A. Linder and G. H. Kutz, "Digital Moving Target Indicators," Supplement to IEEE Trans. on Aerospace and Electronic Systems, Vol. AES-3, No. 6, November 1967, pp. 374-385.

[7] H. L. Van Trees, "Optimum Signal Design and Processing for Reververation-Limited Environments," IEEE Trans. on Military Electronics, Vol. 1, July-October 1965, pp. 212-229.

[8] B. Gold and C. M. Radar, Digital Processing of Signals (McGraw-Hill New York, 1969), Section 4.13.

[9] R. J. McAulay and R. D. Yates, "Realization of the Gauss-in-Gauss Detector Using Minimum-Mean-Squared-Error Filters," IEEE Trans. on Information Theory, Vol. IT-17, No. 2, March 1971, pp. 207-209.

[10] H. L. Van Trees, Detection Estimation and Modulation Theory, Part III, (Wiley, 1971, New York), Chapter 2.

[11] B. Gold and C. M. Radar, op. cit. Section 2.8.

[12] B. C. Kuo, Discrete-Data Control Systems (Prentice Hall, Inc., New Jersey, 1970) pp. 49.

[13] W. D. Wirth, "Detection of Doppler Shifted Radar Signals with Clutter Rejection," AGARD Conference Proceedings No. 66 on Advanced Radar Systems, November 1970, pp. 30-1 to 30-19.

[14] L. E. Brennan and I. S. Reed, "Optimum Processing of Unequally Spaced Radar Pulse Trains for Clutter Rejection," IEEE Trans. on Aerospace and Electronic Systems, Vol. AES-4, No. 3, May 1968, pp. 474-477.

[15] B. C. Kuo, op. cit., Chapter 3.

[16] Air Route Surveillance Radar ARSR-2, Vol. I, General Description and Theory of Operation, Raytheon Company, 1960.

[17] S. E. Perlman, "Staggered Rep Rate Fills Radar Blind Spots," Electronics, 21 November 1958, pp. 82-85.

[18] H. M. Finn and R. S. Johnson, "Adaptive Detection Mode with Threshold Control As A Function of Spatially Sampled Clutter-Level Estimates," RCA Review, September 1968, pp. 414-464.

[19] D. J. Sakrison, R. J. McAulay, V. C. Tyree and J. H. Yuen, "An Adaptive Receiver Implementation for the Gaussian Scatter Channel," IEEE Trans. on Communication Technology, Vol. Com-17, No. 6, December 1969, pp. 640-648.

DOCUMENT CONTROL DATA - R&D

(Security classification of title, body of abstract and indexing annotation must be entered when the overall report is classified)

1. ORIGINATING ACTIVITY *(Corporate author)* Lincoln Laboratory, M.I.T.	2a. REPORT SECURITY CLASSIFICATION Unclassified 2b. GROUP None

3. REPORT TITLE

A Theory for Optimal MTI Digital Signal Processing: Part I. Receiver Synthesis

4. DESCRIPTIVE NOTES *(Type of report and inclusive dates)*

Technical Note

5. AUTHOR(S) *(Last name, first name, initial)*

McAulay, Robert J.

6. REPORT DATE	7a. TOTAL NO. OF PAGES	7b. NO. OF REFS
22 February 1972	70	19

8a. CONTRACT OR GRANT NO. F19628-70-C-0230 b. PROJECT NO. 649L c. d.	9a. ORIGINATOR'S REPORT NUMBER(S) Technical Note 1972-14 (Part I) 9b. OTHER REPORT NO(S) *(Any other numbers that may be assigned this report)* ESD-TR-72-55

10. AVAILABILITY/LIMITATION NOTICES

Approved for public release; distribution unlimited.

11. SUPPLEMENTARY NOTES	12. SPONSORING MILITARY ACTIVITY
None	Air Force Systems Command, USAF

13. ABSTRACT

A classical problem in radar theory is the detection of moving targets in a ground clutter plus receiver noise background. Improvements in clutter rejection have recently been made by replacing analog MTI processors by their digital equivalents as this eliminates many of the problems associated with the maintenance of the analog hardware. In an attempt to determine the ultimate improvements possible using this new technology, the MTI problem was formulated as a classical detection problem and solved using the generalized likelihood ratio test. By manipulating the likelihood ratio, the receiver could be interpreted as a clutter filter in cascade with a doppler filter bank. The performance of the optimum receiver was evaluated in terms of the output signal-to-interference ratio and compared with well-known MTI processors. It was shown that near-optimum performance can be obtained using a sliding weighted Discrete Fourier Transform (DFT).

All of the results in Part I assume uniformly spaced transmitted pulses, which, for high velocity aircraft, leads to aliasing of the target and clutter spectra and detection blind speeds. In Part II the maximum likelihood method is applied using a more general model for the non-uniformly sampled target returns. This leads to an optimum receiver that is a slightly more complicated version of the sliding weighted DFT. In addition to removing the detection blind speeds, it is found that unambiguous doppler measurements are possible by selecting the staggering algorithm to properly design the signal's ambiguity function.

14. KEY WORDS

air traffic control
moving target indication (MTI)
digital signal processing
Fourier transform
clutter rejection filter